

# AIP | The Journal of Chemical Physics

## Quantum stereodynamics of the $\text{Li}+\text{HF}(v,j)$ reactive collision for different initial states of the reagent

Manuel Lara, Alfredo Aguado, Octavio Roncero, and Miguel Paniagua

Citation: *J. Chem. Phys.* **109**, 9391 (1998); doi: 10.1063/1.477600

View online: <http://dx.doi.org/10.1063/1.477600>

View Table of Contents: <http://jcp.aip.org/resource/1/JCPSA6/v109/i21>

Published by the [American Institute of Physics](http://www.aip.org).

### Additional information on *J. Chem. Phys.*

Journal Homepage: <http://jcp.aip.org/>

Journal Information: [http://jcp.aip.org/about/about\\_the\\_journal](http://jcp.aip.org/about/about_the_journal)

Top downloads: [http://jcp.aip.org/features/most\\_downloaded](http://jcp.aip.org/features/most_downloaded)

Information for Authors: <http://jcp.aip.org/authors>

## ADVERTISEMENT

# Instruments for advanced science

### Gas Analysis



- dynamic measurement of reaction gas streams
- catalysis and thermal analysis
- molecular beam studies
- dissolved species probes
- fermentation, environmental and ecological studies

### Surface Science



- UHV TPD
- SIMS
- end point detection in ion beam etch
- elemental imaging - surface mapping

### Plasma Diagnostics



- plasma source characterization
- etch and deposition process reaction kinetic studies
- analysis of neutral and radical species

### Vacuum Analysis



- partial pressure measurement and control of process gases
- reactive sputter process control
- vacuum diagnostics
- vacuum coating process monitoring

contact Hiden Analytical for further details

**HIDEN**  
ANALYTICAL

[info@hideninc.com](mailto:info@hideninc.com)  
[www.HidenAnalytical.com](http://www.HidenAnalytical.com)

CLICK to view our product catalogue 

# Quantum stereodynamics of the $\text{Li}+\text{HF}(v,j)$ reactive collision for different initial states of the reagent

Manuel Lara, Alfredo Aguado,<sup>a)</sup> and Octavio Roncero

*Instituto de Matemáticas y Física Fundamental, C.S.I.C., Serrano 123, 28006 Madrid, Spain*

Miguel Paniagua

*Departamento de Química Física, Facultad de Ciencias C-XIV, Universidad Autónoma de Madrid, 28049 Madrid, Spain*

(Received 9 July 1998; accepted 28 August 1998)

The effect of the reagent initial state excitation on the reactive cross section in the  $\text{Li}+\text{HF}(v,j)$  collision is analyzed for  $v=0, 1$  and  $j=0, 1, 2$  and  $3$ . A wave packet treatment is used within the centrifugal sudden approximation on a global potential energy surface recently proposed [Aguado *et al.*, *J. Chem. Phys.* **107**, 10085 (1997)]. The reaction cross-section for  $v=0$  is in good agreement with the available experimental data, and for low  $j$  shows oscillations as a function of the translational energy which are due to the structure of the transition state. For  $v=1$  the reaction cross-section increases by a factor of 10–50 with respect to that of  $v=0$ . The influence of the alignment of the initial angular momentum on the reaction cross section is studied. © 1998 American Institute of Physics. [S0021-9606(98)02345-9]

## I. INTRODUCTION

The influence of the initial excitation of the reactants on the reaction probability provides information on the potential energy surface (PES) and on the reaction mechanisms. Alkali or alkaliearth atoms ( $M$ ) with hydrogen halide molecules ( $HX$ ) are good examples for which there are many experimental studies determining the effects of reagent excitation vibrational,<sup>1–5</sup> rotational<sup>6–10</sup> and electronic<sup>11–14</sup> excitation. It is particularly interesting the determination of the role of the transition state on the reaction dynamics, mainly for energies close to the threshold, and the  $M+HX$  systems present a wide variety of situations, the reactions being endothermic, exothermic or thermoneutral depending on the nature of the metal atom ( $M$ ) and of the hydrogen halide molecule ( $HX$ ), and on the initial excitation of the reactants. Nowadays, there is an increasing number of theoretical works on these systems<sup>15–20</sup> due to the development of the methodology to describe the reaction dynamics of three atoms systems and to the appearance of accurate global potential energy surfaces (GPES) for some of these systems like  $\text{Li}+\text{HF}$ <sup>16,19</sup> or  $\text{Na}+\text{HF}$ .<sup>20–22</sup>

Another source of valuable information is the reaction dynamics dependence on the relative velocity vectors between reactants and products and on the angular momenta involved in the process. This means that it is necessary to create and register the relative orientation of the different vector properties involved in a reactive collision, and their mutual correlations, to get a deeper insight about the reaction dynamics.<sup>23–26</sup> In this regard, several experimental studies have been done in  $M+HX$  systems to determine the influence of the alignment of the reagent molecule on the reaction,<sup>27–30</sup> which provides valuable information about the

potential energy surface on the entrance valley, as well as on the final rotational polarization of the product molecule.<sup>31,32</sup>

The reactions of  $M+HX$  systems are envisaged as harpoon-type processes, and the ground electronic state of these systems is a result of a curve crossing between an ionic ( $M^+ + HX^-$ ) and a covalent ( $M+HX$ ) diabatic states. This crossing is frequently the responsible of the appearance of the barrier along the reaction path. The determination of the structure of the transition state is of great importance since it determines important features of the reaction mechanism. A method for the direct spectroscopic investigation of the transition state is the study of the photoinitiated reaction from the van der Waals complex of the reactants.<sup>33–40</sup> In these kinds of experiments on  $M+HX$  systems, the complex is promoted to an excited electronic state of the metal atom,<sup>34–40</sup> and the generated product fragments detected show a certain rotational polarization due to the relative orientation of the reactants in the van der Waals complex. Moreover, in a recent work<sup>41</sup> we have shown the possibility of accessing the vicinity of the transition state on the ground electronic state by infrared excitation of the complex of  $\text{Li-HF}$ , obtaining a high efficiency in forming  $\text{LiF}$  products at total energies where the collisional reaction cross section is rather low. Even when this last study was devoted to the particular case of  $\text{Li-HF}$ , it is found that this possibility is based on rather general properties of  $M+HX$  systems: a sudden change of the electric dipole moment near the transition state (a consequence of the curve crossing mentioned above), and a well in the reactant valley at configurations relatively close to the saddle point. In fact, the experimental detection of the products in the photoinitiated reaction of  $\text{Li-HF}$  presents some disadvantages since this system reacts at thermal energies. However, other related systems like  $\text{Na-HF}$ <sup>20–22</sup> and  $\text{Ca-HF}$ <sup>42</sup> have a higher reaction threshold and deep wells in the reactants valley that make them good

<sup>a)</sup>Permanent address: Departamento de Química Física, Facultad de Ciencias C-XIV, Universidad Autónoma de Madrid, 28049 Madrid, Spain.

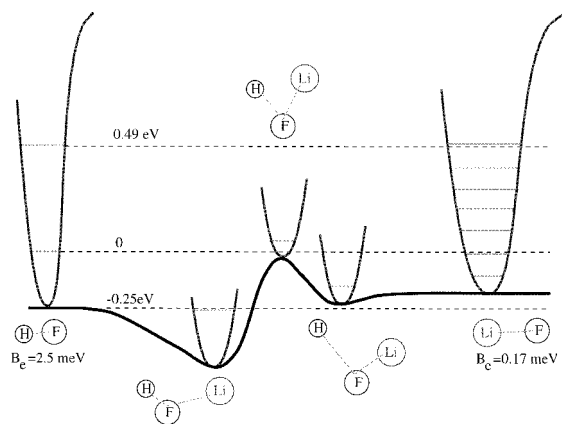


FIG. 1. Energy diagram of the reaction path for  $\text{Li}+\text{HF}\rightarrow\text{LiF}+\text{H}$  collision using the GPES of Ref. 19.

candidates for such experiments on the ground electronic state.

$\text{Li}+\text{HF}$  is becoming a benchmark for theoretical calculations because its relative low number of electrons allows highly accurate *ab initio* calculations on the ground electronic state,<sup>43,44</sup> and recently several global PES's have been published.<sup>16,19</sup> In addition, there are molecular beam experiments for  $\text{HF}(v=0)$ <sup>45</sup> as well as experiments on the influence of the initial alignment of  $\text{HF}(v=1, j=1)$  on the reaction.<sup>46,30</sup> In this work we study the effect of the initial state excitation of the reactants on the  $\text{Li}+\text{HF}(v, j)$  reactive collision, placing special emphasis on the correlation between the relative velocity of reactants and the rotational polarization of HF. We use a global PES recently published by us<sup>19</sup> whose main features are shown in Fig. 1. The reaction dynamics is studied with a time-dependent treatment within a body-fixed frame<sup>19</sup> using the centrifugal sudden approximation, which is described in Sec. II. In Sec. III the results are discussed and, finally, the last section is devoted to some conclusions.

## II. QUANTUM TIME-DEPENDENT REACTIVE DYNAMICS

In the present work the reaction dynamics is studied using a wave packet treatment described previously in detail,<sup>19</sup> and only a brief description is included here. Reactant Jacobi coordinates are used in which  $\mathbf{r}$  is the HF internuclear vector,  $\mathbf{R}$  is the vector joining the center of mass of HF to the Li atom, and  $\gamma$  is the angle between them. It is convenient to use a body-fixed frame, such that the  $z$ -axis lies along the  $\mathbf{R}$  vector and all three atoms lie in the  $x$ - $z$  plane, to distinguish between the internal coordinates,  $r$ ,  $R$  and  $\gamma$ , and three Euler angles  $\theta$ ,  $\phi$  and  $\chi$  specifying the orientation of the body-fixed axes with respect to the space-fixed frame.<sup>47</sup> In this representation the total wave packet is expanded as,

$$\Psi^{JM}(\mathbf{R}, \mathbf{r}, t) = \sum_{\Omega} \sqrt{\frac{2J+1}{8\pi^2}} \times D_{M\Omega}^{J*}(\phi, \theta, \chi) \frac{\Phi_{\Omega}^{JM}(r, R, \gamma, t)}{rR}, \quad (1)$$

where the  $D_{M\Omega}^J$  are Wigner rotation matrices<sup>47</sup> corresponding to a total angular momentum  $J$ , associated with the total angular operator  $\hat{\mathbf{J}} = \hat{\mathbf{j}} + \hat{\mathbf{I}}$  (with  $\hat{\mathbf{j}}$  and  $\hat{\mathbf{I}}$  being the angular momentum operators associated with  $\mathbf{r}$  and  $\mathbf{R}$ , respectively).  $M$  and  $\Omega$  are the projections of  $\mathbf{J}$  on the space-fixed and body-fixed  $z$ -axis, respectively. Since the  $z$ -axis is parallel to  $\mathbf{R}$ ,  $\Omega$  is also the projection of  $\mathbf{j}$ , the angular momentum of diatomic reagent.

Different  $\Omega$  projections are coupled by Coriolis, associated with the  $\hat{\mathbf{I}}^2$  term appearing in the Hamiltonian operator. To converge the reaction cross sections it is necessary to perform calculations up to high  $J$ , typically of the order of 80 for some of the cases discussed below. Due to the difficulty of performing exact calculations, i.e., including all possible  $\Omega$  values, for such high  $J$ , some approximation should be done. In this work we use the centrifugal sudden approach (CSA),<sup>48-50</sup> in which the Coriolis coupling between different  $\Omega$  values is neglected and, hence, the sum over  $\Omega$  in Eq. (1) is limited to a single value. In a previous work, total reaction probabilities obtained using the centrifugal sudden approach (CSA) were found to be in excellent agreement with an "exact" calculation made for  $J=5$  (including all possible  $\Omega$  projections). This is due to two main reasons. First, the total reaction probabilities are averaged quantities and seem to be nearly insensitive to this approximation. However, for other magnitudes, such as partial or differential cross sections, this approximation is not expected to work as well, and it should be checked. Second, the hydrogen atom is so light, compared to F and Li atoms, that the complete system is analogous to a diatomic molecule formed by the HF "superatom" and Li atom, provided that the H atom is close to the F atom. This last condition is fulfilled in the reactants valley and explains why the CSA works so well for the total reaction probability. The situation in the products valley, however, is different because the hydrogen atom gets far away from the LiF molecule.

The integration of the time-dependent Schrödinger equation is performed using the Chebyshev method<sup>51</sup> and the  $\Phi_{\Omega}^{JM}(r, R, \gamma, t)$  coefficients are represented on finite grids for the internal coordinates  $r$ ,  $R$ ,  $\gamma$ . A set of equidistant points,  $r_n, R_m$ , is chosen for the two-dimensional radial grid, and the radial kinetic term is solved using the fast Fourier transform method.<sup>52</sup> In order to avoid artificial reflections, due to the use of a finite grid, the wave packet is absorbed after each time step.<sup>19</sup> For  $\gamma$ , we use a set of 25-30 Gauss-Legendre quadrature points,  $\gamma_k$ , with weights  $w_k$ . The action of the angular momentum operators on the wave packet, diagonal in the radial grid representation, is performed in a single operation as a multiplication of a matrix by a vector, as explained previously.<sup>19</sup>

The wave packet at  $t=0$  is defined by the product

$$\Psi^{JM}(\mathbf{R}, \mathbf{r}, t=0) = \sqrt{\frac{2J+1}{8\pi^2}} D_{M\Omega}^{J*}(\phi, \theta, \chi) \times Y_{j,\Omega}(\gamma, 0) \frac{\phi_{v,j}(r)}{r} \frac{G(R)}{R}, \quad (2)$$

where  $\phi_{v,j}(r)$  is the radial part of an eigenstate of  $\text{HF}(v, j)$ ,

$Y_{j,\Omega}$  is a spherical harmonic and  $G(R)$  is a complex Gaussian function, centered at an initial value  $R_0=13$  Å, in the asymptotic region, with an approximate mean kinetic energy of  $\approx 0.2$  eV and an energy dispersion of one third of the initial mean kinetic energy.

The energy-resolved total reaction probability is calculated from the total flux of the energy projection of the wave packet through a surface in the products region at  $r^*=3$  Å as<sup>53,54</sup>

$$P_{v,j,\Omega}^J(E) = \frac{\hbar^2 k_{vj}(E)}{4\pi^2 \mu m} \sum_{\Omega} \int dR \sin \gamma d\gamma \times \text{Im} \left[ \Psi_{\Omega}^{+*}(r^*, R, \gamma, E) \frac{\partial \Psi_{\Omega}^+(r, R, \gamma, E)}{\partial r} \Big|_{r^*} \right], \quad (3)$$

where  $k_{vj}(E) = \sqrt{2\mu(E - E_{v,j})}/\hbar$ . The time-independent wave functions  $\Psi_{\Omega}^+$  are defined as

$$\Psi_{\Omega}^+(r, R, \gamma, E) = \frac{1}{a_{vj}(E)} \int_{-\infty}^{\infty} dt e^{iEt/\hbar} \Phi_{\Omega}^{JM}(r, R, \gamma, t), \quad (4)$$

where

$$a_{vj}(E) = \frac{1}{2\pi} \int dR \mathcal{H}_{j\Omega}^{JM*}(k_{vj}R) G(R) \quad (5)$$

is proportional to the initial flux in the entrance channel.  $\mathcal{H}_{j\Omega}^{JM}(k_{vj}R)$  is a body-fixed Bessel function<sup>55</sup> defined as

$$\mathcal{H}_{j\Omega}^{JM}(k_{vj}R) = \sum_{m_{\ell} m_j} T_{\ell m_{\ell} m_j}^{JM\Omega} k_{vj}R h_{\ell}^{(2)}(k_{vj}R), \quad (6)$$

where  $h_{\ell}^{(2)}$  is a spherical Bessel function of the third kind,<sup>56</sup> which asymptotically behaves as  $h_{\ell}^{(2)} \sim_{R \rightarrow \infty} e^{-i(k_{vj}R - \ell\pi/2)}/k_{vj}R$ . Finally, in Eq. (6), the  $T_{\ell m_{\ell} m_j}^{JM\Omega}$  coefficients arise from the transformation from the body-fixed frame to the space-fixed frame and are of the form

$$T_{\ell m_{\ell} m_j}^{JM\Omega} = (-1)^{M-\Omega} \sqrt{(2\ell+1)(2J+1)} \times \begin{pmatrix} \ell & j & J \\ m_{\ell} & m_j & -M \end{pmatrix} \begin{pmatrix} \ell & j & J \\ 0 & \Omega & -\Omega \end{pmatrix}. \quad (7)$$

From the reaction probabilities, the reaction cross section, for a particular initial  $(v, j)$  state of the reactants, is defined as

$$\sigma_{v,j}(E) = \frac{1}{2j+1} \sum_{\Omega=-j}^j \sigma_{v,j,\Omega}(E), \quad (8)$$

where an isotropic distribution of the vector  $\mathbf{j}$  is assumed. The information about the influence of the initial direction of the  $\mathbf{j}$  vector with respect to the relative velocity vector between reactants, which coincides with the body-fixed  $z$ -axis in the present treatment, is in the helicity dependent cross sections,  $\sigma_{v,j,\Omega}$ , defined as

$$\sigma_{v,j,\Omega}(E) = \frac{\pi}{k_{vj}^2} \sum_{J=\Omega}^{\infty} (2J+1) P_{vj\Omega}^J(E), \quad (9)$$

since  $\Omega$  is the projection of the  $\mathbf{j}$  and  $\mathbf{J}$  vectors on the body-fixed  $z$ -axis. In addition, knowing that the three particles are in the body-fixed  $x$ - $z$  plane, which rotates in space, for a particular initial  $j, \Omega$  value it is simple to determine the initial orientation of the diatomic axis with respect to the  $z$ -axis through the corresponding spherical harmonic  $Y_{j\Omega}(\gamma, 0)$ . In particular, for  $\Omega=j$  the initial diatomic axis distribution is predominantly perpendicular to  $\mathbf{R}$ , while for  $\Omega=0$  it is parallel. The  $\sigma_{v,j,\Omega}$  contains then valuable information about the  $\mathbf{k}$ - $\mathbf{j}$  correlation which describes part of the stereodynamics of atom-diatom reactions. Sometimes, especially for high  $j$ , it is convenient to express the  $2j+1$  values of  $\sigma_{v,j,\Omega}$  in terms of state multipoles, whose components provide the relative contributions of different polarization of  $\mathbf{j}$  on the reaction.<sup>25,26</sup> The monopole moment is proportional to  $\sigma_{v,j}$ , the isotropic contribution, while all the odd terms vanish in the CSA because  $\sigma_{v,j,\Omega} = \sigma_{v,j,-\Omega}$ . The quadrupole moment provides information about the plane of rotation, and in this work we shall define its proportional quantity

$$\mathcal{A}_{v,j}(E) = \sum_{\Omega} \left[ \frac{3\Omega^2}{j(j+1)} - 1 \right] \rho_{v,j,\Omega}, \quad (10)$$

with  $\rho_{v,j,\Omega} = \sigma_{v,j,\Omega} / \sum_{\Omega} \sigma_{v,j,\Omega}$ . This quantity provides the information about the preferred initial alignment of  $\mathbf{j}$  with  $\mathbf{R}$  to produce the reaction and is analog to the rotational alignment parameter frequently used in photodissociation.<sup>47</sup> For high  $j$ , the semiclassical limit can be used in which  $\cos \theta_j = \Omega / \sqrt{j(j+1)}$  ( $\theta_j$  being the angle between  $\mathbf{j}$  and the  $z$ -axis), and  $\mathcal{A}_{v,j}(E) \propto \langle 2P_2(\cos \theta_j) \rangle$  provides an idea of the most favorable angle between  $\mathbf{j}$  and  $\mathbf{R}$  that yields to the products. In the semiclassical limit, the  $\mathcal{A}_{v,j}$  parameters take values between  $-1$  and  $2$ .  $\mathcal{A}_{v,j} = -1$  and  $2$  means that the reaction is more probable when  $\mathbf{j}$  is perpendicular or parallel to the  $z$ -axis, respectively, while  $\mathcal{A}_{v,j} = 0$  means that the reaction is independent of  $\Omega$ .

### III. RESULTS AND DISCUSSIONS

#### A. Transition state structure and reaction probabilities

Some of the features of the reaction dynamics are imposed by the PES in the neighborhood of the saddle point, the point of no return, which for the case of Li+HF shows two major features, as it is shown in Fig. 2. First, the saddle point is located in the exit channel, at HF internuclear distance,  $r$ , longer than that of free HF. Second, the minimum energy reaction path is along the  $r$  coordinate at the transition state, and the contour plot of the PES at  $r_{TS}=1.301$  Å (the position of the saddle point in the HF internuclear distance), as a function of  $R$  and  $\gamma$ , in Fig. 2(b), presents a local minimum. These features indicate that this system presents a ‘‘late barrier’’<sup>57,58</sup> for which the reaction efficiency increases with initial vibrational excitation of HF rather than with the translational energy, as will be discussed later. Moreover, the ‘‘bound’’ states on the coordinates perpendicular to the reaction path, i.e., the other two internal coordinates  $R$  and  $\gamma$  and the three Eulerian angles  $\phi, \theta, \chi$ , introduce certain structure on the reaction probabilities, as it is

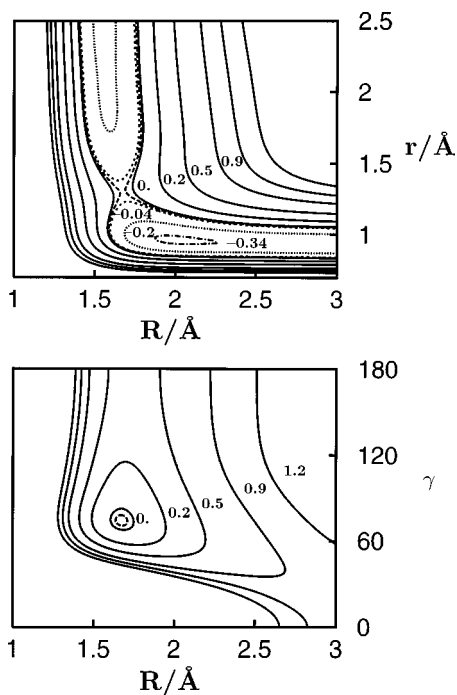


FIG. 2. Contour plot of the GPES of Ref. 19 at the saddle point (which is located at  $r=1.301$  Å,  $R=1.672$  Å and  $\gamma=73.53^\circ$ ). (a) For  $\gamma=73.53^\circ$  and (b) for  $r=1.301$  Å. Energy is referred to the HF( $v=0, j=0$ ) eigenvalue.

discussed below. In order to calculate these “bound” states, we consider the approximated Hamiltonian at the transition state as

$$H^{TS} = -\frac{\hbar^2}{2m} \left( \frac{2}{R} \frac{\partial}{\partial R} + \frac{\partial^2}{\partial R^2} \right) + \frac{\ell^2}{2mR^2} + \frac{j^2}{2\mu r_{TS}^2} + V(r_{TS}, R, \gamma), \quad (11)$$

which arises from the exact Hamiltonian in these coordinates (including all the Coriolis term) freezing  $r=r_{TS}$ .

The “bound” states are expanded in a basis set of the type

$$\Psi_n^{JM}(\mathbf{R}, \hat{r}) = \sum_{\Omega, j, m} A_{\Omega, j, m}^{JMn} \sqrt{\frac{2J+1}{8\pi^2}} D_{M\Omega}^{J*}(\phi, \theta, \chi) \times Y_{j\Omega}(\gamma, 0) \varphi_m(R), \quad (12)$$

where  $Y_{j\Omega}$  is a spherical harmonic and  $\varphi_m$  is a numerical radial basis set function obtained by solving a monodimensional Hamiltonian using a reference potential chosen to minimize the number of radial basis set functions in the diagonalization. The eigenvalues obtained for  $J=0$  and 1 are shown in Table I, referred to the energy of HF( $v=0, j=0$ ). The first eigenvalue is at positive energies and explains that the reaction cross section obtained for Li+HF( $v=0, j=0$ )<sup>19</sup> shows a threshold when the zero-point energy at the transition state is included. In addition, the reaction probabilities obtained for Li+HF( $v=0, j, J=0$ )<sup>19</sup> for several  $j$  values show an oscillating envelope superimposed to a highly structured resonant region, at low energies, that disappears at higher energies. The resonances are mainly attributed to the deep well in the reactants valley.

TABLE I. “Bound” levels at the saddle point obtained by freezing the HF internuclear distance to its value at the saddle point. Energies are in eV. For  $J=1$  the states of total parity  $p=(-1)^j$  are listed, and the main  $\Omega$  component (and its weight) is shown. This weight is evaluated as  $w_\Omega = \sum_{m,j} |A_{\Omega, j, m}|^2$ . The levels of the other parity for  $J=1$  are nearly degenerate with those with a dominant weight on  $\Omega=1$  and are not shown in the table.

$n$	$J=0$	$J=1$	
	$E_n$	$E_{n\Omega}$	$\Omega$ ( $w_\Omega$ )
0	0.0688	0.0691	0 (0.9990)
1	0.1487	0.0703	1 (0.9990)
		0.1490	0 (0.9989)
2	0.1560	0.1503	1 (0.9986)
		0.1562	0 (0.9987)
3	0.2211	0.1575	1 (0.9990)
		0.2213	0 (0.9990)
4	0.2307	0.2226	1 (0.9988)
		0.2309	0 (0.9986)
5	0.2412	0.2322	1 (0.9985)
		0.2415	0 (0.9988)
6	0.2834	0.2428	1 (0.9990)
		0.2837	0 (0.9985)
7	0.3032	0.2851	1 (0.9984)
		0.3034	0 (0.9987)
8	0.3107	0.3047	1 (0.9981)
		0.3110	0 (0.9979)
9	0.3245	0.3123	1 (0.9983)
		0.3247	0 (0.9988)
		0.3260	1 (0.9989)

The maxima of the oscillating envelope are located at total energies close to the “bound” states of the transition state (see Fig. 3). The “bound” states at the saddle point are slightly shifted toward higher energies than the maxima of the reaction probabilities. This shift is due to the coupling of the “bound” states to the continuum on the reaction path coordinate. It should be noted that the intensity of the maxima decreases with increasing the rotational excitation, but even for  $j=3$  there are small structures that can also be associated to the “bound” states at the saddle point. For the particular case of  $j=2$ , the oscillations are less intense than for the rest, and as a consequence the reaction probability is significantly lower in the energy interval dominated by the oscillations.

For  $J=1$  the levels split in two, each one with a nearly pure  $|\Omega|$  value (with a weight of  $\approx 0.99$ ) which confirms that the CSA is reasonable to study the reaction dynamics. The energy differences between the two  $\Omega=0$  and 1 “bound” levels is of the order of 1 meV. However, the reaction probabilities for the Li+HF( $v=0, j=1, J=1$ ) collision, in Fig. 4, the maxima for  $|\Omega|=0$  and 1 are shifted by  $\approx 10$ -20 meV. In order to explain this apparent disagreement between the shifts, it should be noted that at high energies, where the oscillations disappear, the reaction probability for the case  $\Omega=0$  is about four times larger than that of  $|\Omega|=1$ , which means that there are strong steric effects. Therefore, the coupling of the “bound” states at the saddle point with the corresponding reaction path continua for each  $\Omega$  must be different for the two cases, and this fact could explain why for  $\Omega=0$  the maxima are shifted toward lower energies, as in

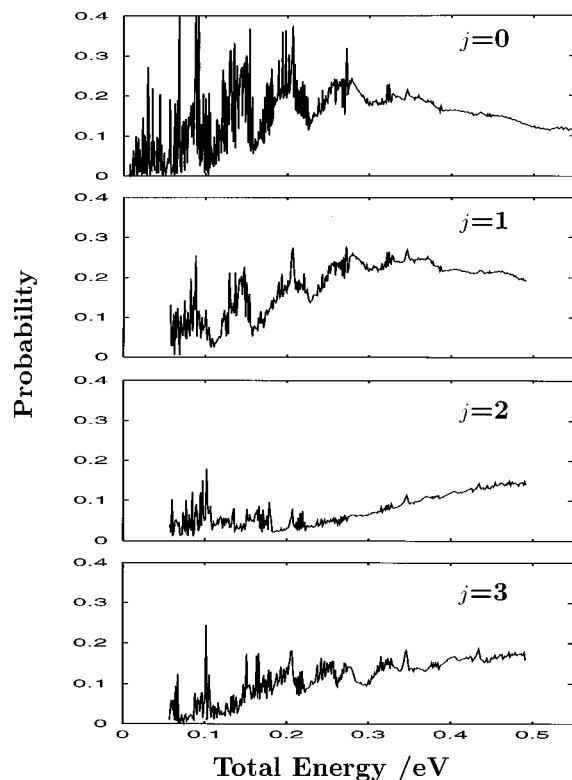


FIG. 3. Reaction probabilities for the  $\text{Li}+\text{HF}(v=0, j=0, 1, 2, \text{ and } 3, J=0)$  collision as a function of total energy, referred to the eigenvalue of  $\text{HF}(v=0, j=0)$ , from Ref. 19.

the  $J=0$  case discussed above, while for  $|\Omega|=1$  the shift is toward higher energies. As it will be discussed below, this fact has an important influence on the stereodynamics of the reaction.

For higher values of the total angular momentum, the reaction probabilities for  $\text{HF}(v=0, j=1, J, \Omega)$  show a simi-

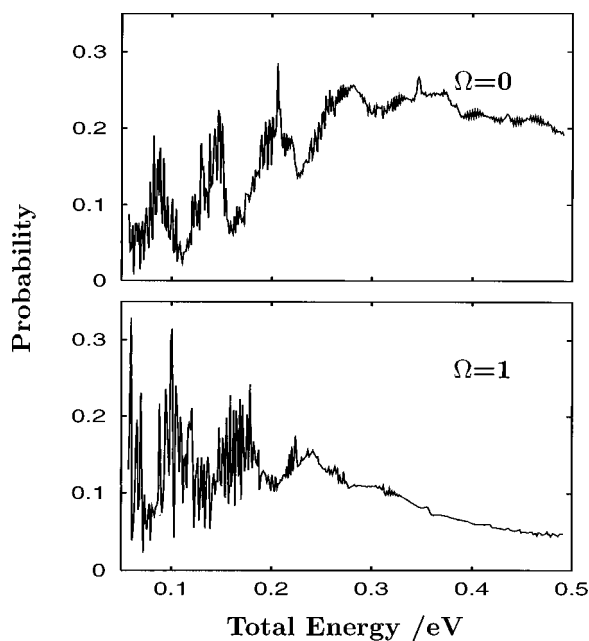


FIG. 4. Reaction probabilities for the  $\text{Li}+\text{HF}(v=0, j=1, J=1, \Omega)$  collision as a function of total energy.

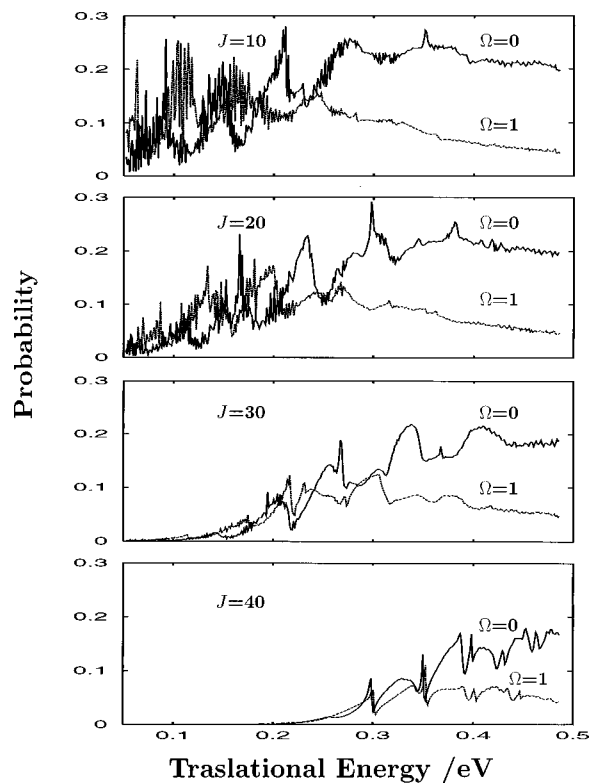


FIG. 5. Reaction probabilities for the  $\text{Li}+\text{HF}(v=0, j=1, J, \Omega)$  collision as a function of translational energy for several  $J$ 's, obtained within the CSA.

lar behavior to that discussed for  $J=1$ , as it is shown in Fig. 5. The probabilities as a function of  $J$  for a fixed value of  $\Omega$  show a shift, approximately consistent with the increase of the rotational barrier at the saddle point, and an overall decrease. However, the relation between the reaction probabilities for different  $\Omega$  values is not simple for this case. The same situation occurs for  $j=2$  and  $3$ , whose reaction probabilities for  $J=30$  are shown in Figs. 6 and 7, respectively.

## B. Effect of the rotational excitation of the reactants

The total reaction cross section for  $\text{Li}+\text{HF}(v=0, j)$ , obtained with Eq. (8), where an isotropic distribution of the diatomic reactant is assumed, is shown in Fig. 8(a), and compared with the available experimental data of Becker *et al.*<sup>45</sup>

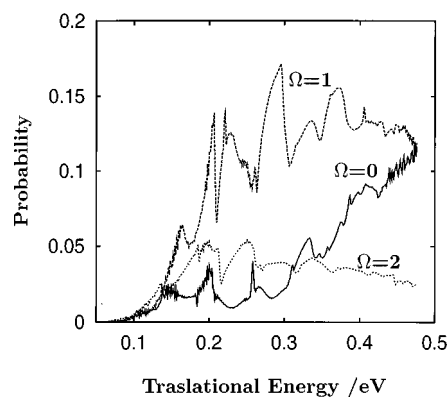


FIG. 6. Reaction probabilities for the  $\text{Li}+\text{HF}(v=0, j=2, J=30, \Omega)$  collision.

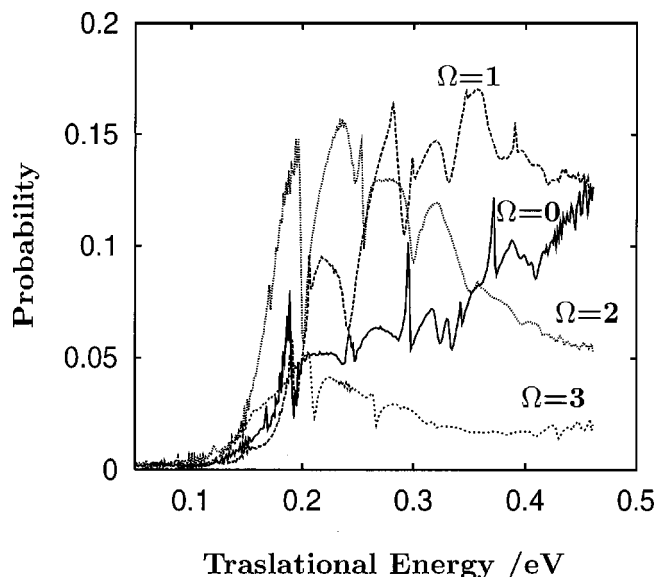


FIG. 7. Reaction probabilities for the Li+HF( $v=0, j=3, J=30, \Omega$ ) collision.

All the reaction cross sections are inside the experimental error bars, which demonstrates the goodness of the GPES used.<sup>19</sup> At low translational energies the cross section for  $j=0$  shows oscillations that, as discussed above, are due to the structure of the transition state. For  $j=1$  the oscillations at low energy are absent due to the average over  $\Omega=0$  and 1, the associated reaction probabilities of which are shown in

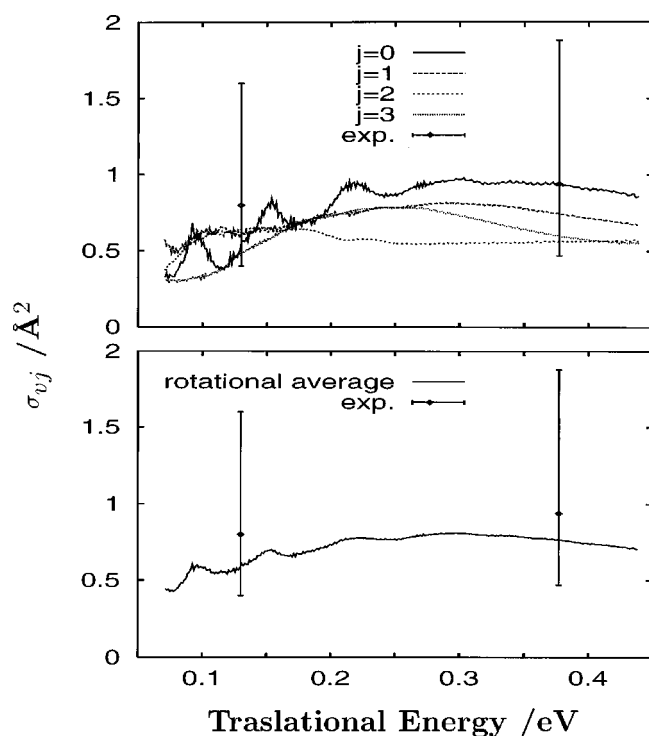


FIG. 8. (a) Reaction cross-section for the Li+HF( $v=0, j$ ) reactive collision for  $j=0, 1, 2$ , and 3, and (b) reaction cross section averaged over several initial rotational states of HF( $v=0$ ) with weights being 0.314, 0.465, 0.189 and 0.032 for  $j=0, 1, 2$ , and 3, respectively, as determined in infrared fluorescence experiments (Ref. 59) at typical rotational temperatures of 60–80 K.

Fig. 5. For  $j=2$  and 3 there are no oscillations in the total reaction cross sections at low translational energies.

The oscillations provide good information about the PES in the saddle point, and it is interesting to check if they persist after rotational average, with typical rotational temperatures obtained in molecular beam experiments ( $\approx 60$ – $80$  K). For this reason, in the rotational average we use the weights 0.314, 0.465, 0.180 and 0.032 for  $j=0, 1, 2$  and 3, respectively, which have been measured in an HF beam with the infrared fluorescence technique.<sup>59</sup> The result of such rotational averages, in Fig. 8(b), shows that the oscillations persist, but with less intensity, and that the theoretical cross section values are again in good agreement with the few experimental data available. We conclude that in this respect it would be interesting to perform experimental measurements of the reaction cross section at several energies, especially at low energies, since the detection of the oscillations would provide a direct information on the PES in the region of the saddle point.

At high energies, the reaction cross sections are more regular. There is a decrease of the cross section when increasing the initial rotational excitation of HF. At intermediate energies, however, the cross section for  $j=3$  is larger than those for  $j=1$  and 2. There have been several experimental studies on the effect of the rotational excitation on the reactivity in related systems, like Na+HF,<sup>6</sup> K+HF,<sup>7</sup> K+HCl,<sup>8</sup> Sr+HF,<sup>9,10</sup> and Ca+HF,<sup>10</sup> in which it is found that the reaction cross section shows an initial decline followed by a subsequent rise with increasing  $j$ , in analogy to what we find for Li+HF( $v=0$ ). In most of them the  $HX$  reagent is prepared in a vibrationally and rotationally excited state, but usually these systems present a saddle point at larger energies so that the study is done close to the threshold, as in the case of Li+HF in  $v=0$ .

Several models have been proposed to understand the role of initial rotation of reagents in reactivity,<sup>60–62</sup> and the effect already mentioned has been sometimes explained in terms of the so-called “rotational sliding mass model.”<sup>61</sup> In this model, the internuclear distance of the HF diatomic molecule is considered rigid until its distance to the Li atom gets to a certain critical distance where it is considered that the reaction takes place. Since at energies close to the threshold the saddle point corresponds to a very narrow angular passage, the reaction is strongly hindered in the absence of re-orientation during the approach of the reactants. The anisotropy of the PES exerts torques that drive the system to the region of minimum energy, making it possible for the reagents to get close enough to react. Torques will be increasingly less effective the higher the translational or rotational energy. This effect explains the disruption of the reactivity by the rotational excitation. The subsequent increase can be attributed to favorable excitation of bending in the transition state when the rotational angular momentum of HF and the orbital angular momentum of Li with respect to HF compensate, which helps to overcome the barrier. This traditional explanation of the rotational effect will be somehow changed later on in the section devoted to the analysis of the steric effects on this reaction.

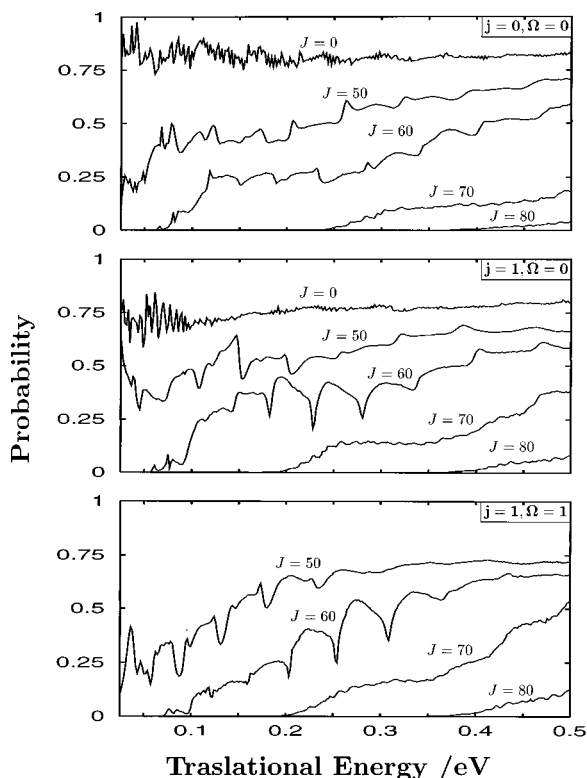


FIG. 9. Reaction probabilities for the Li+HF( $v=1$ ) collision and (a)  $j=0$ ,  $J, \Omega=0$ , (b)  $j=1$ ,  $J, \Omega=0$  and (c)  $j=1$ ,  $J, \Omega=1$ , as a function of translation energy, obtained within the CSA.

### C. Effect of the vibrational excitation of the reactants

The reaction probabilities for Li+HF( $v=1, j=0, 1$ ) for several  $J$  and  $\Omega$  values, in Figs. 9, show important differences with those obtained for  $v=0$ . First of all, the reaction probabilities for  $v=1$ , of the order of 80%–90%, are about four to five times higher than those obtained for  $v=0$ . The vibrational frequency of HF is  $\approx 0.5$  eV, so that the energies accessible for  $v=1$  are much higher than the saddle point. The total energy at low translational energies for  $v=1$  in Figs. 9 is comparable to that of  $v=0$  at 0.5 eV, in Fig. 5, and the reaction probabilities at the same total energies are very different. Therefore, the high reactivity in the case of  $v=1$  is not simply a question of total energy. The major factor is the higher vibrational excitation of HF that produces an enhancement of the reactivity, as expected for “late barrier” systems,<sup>57,58</sup> as is the situation for LiHF [see Fig. 2(a)]. Therefore, it can be argued that the low reaction cross section for  $v=0$  is due to the fact that during the approach of the reactants, HF does not get enough vibrational excitation to overpass the barrier, some initial vibrational excitation in the HF being necessary.

In contrast to what happens in the  $v=0$  case, the reaction probabilities for  $v=1$  and different  $\Omega$  values are very similar, which already suggests that there are not strong steric effects. In addition, the reaction probabilities for  $j=0$  and 1 are very similar. The absence of rotational disruption at these energies is not surprising since the angular cone of acceptance of the reaction is wider than in the case of  $v=0$ . The total reaction cross section for  $v=1$  and  $j=0$  and

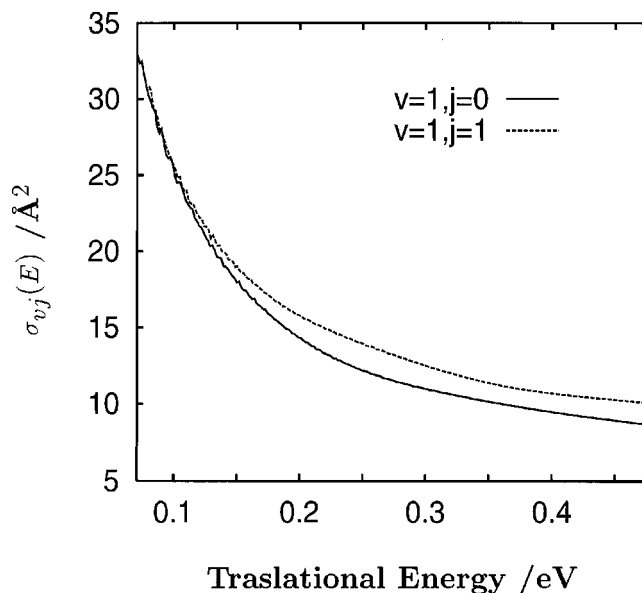


FIG. 10. Total reaction cross section for the Li+HF( $v=1, j=0$  and 1).

1 are shown in Fig. 10 and they look pretty much the same.

These reaction cross sections are about 10 to 50 times larger than those for  $v=0$  at the same translational energies. This factor in the cross section is increased with respect to the equivalent one between the reaction probabilities because the number of partial waves is considerably increased for  $v=1$ . This large enhancement of the reaction with initial vibrational excitation of the reagents has been observed experimentally for some related systems, like K+HCl,<sup>1</sup> Ba+HF,<sup>2</sup> Ca+HF,<sup>3,10</sup> Sr+HF,<sup>3,4,10</sup> and Na+HF.<sup>4</sup> Most of these systems are endothermic for  $v$ , while Li+HF is nearly thermo-neutral, but this difference does not seem to make important differences.

The monotonous decrease of the reaction cross section with increasing translational energy is the typical situation of exothermic reaction with no barrier.<sup>63,64</sup> Using the simple Langevin model for the case of no barrier and for potentials of long range asymptotic form  $V(R) \propto -R^{-s}$ , the reaction cross section behaves as  $\sigma \propto E^{-2/s}$ .<sup>63,64</sup> When the cross sections of Fig. 10 are fitted to such expressions, we get for low energies that  $s=3$ . Taking into account that the asymptotic behavior of the potential describing the Li + HF interaction is  $\propto -R^{-6}$ , this result of  $s=3$  is rather surprising. Since the PES is rather anisotropic in the entrance channel there should be strong steric restrictions to apply directly such a simple model. However, the qualitative decreasing behavior is well understood when using this Langevin model.<sup>64</sup>

### D. Stereodynamics

The helicity dependent cross section,  $\sigma_{v,j,\Omega}(E)$  given in Eq. (9), provides all the information about the dependence of the reactivity on the direction of the initial angular momentum  $\mathbf{j}$  with respect to the relative velocity between reactants, which in the present treatment coincides with the body-fixed  $z$ -axis, i.e., the  $\mathbf{k}\text{-}\mathbf{j}$  correlations. In the CSA  $\sigma_{v,j,|\Omega|}(E) = \sigma_{v,j,-|\Omega|}(E)$  and no difference can be established between different senses of rotations or, in other words, all the odd



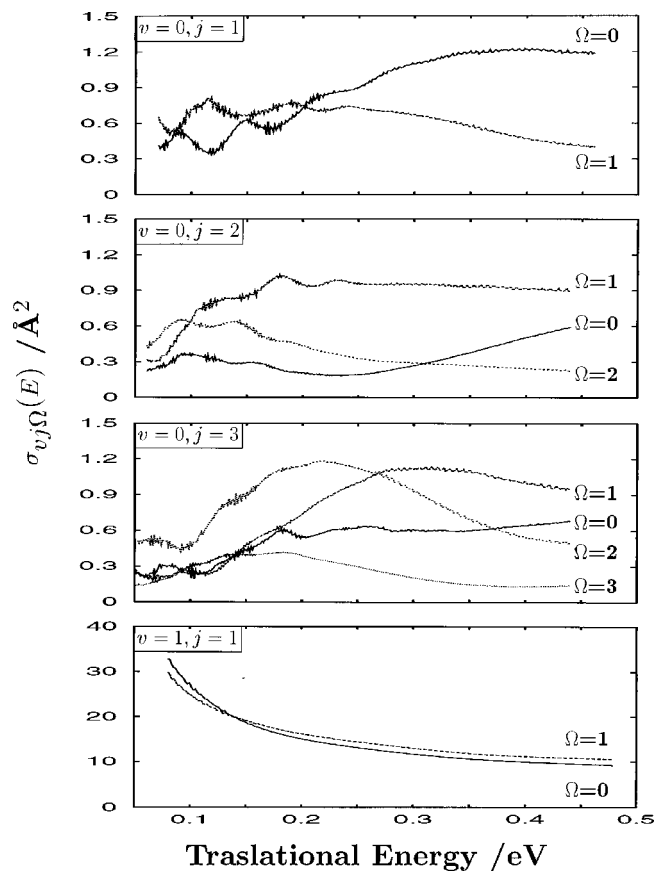


FIG. 11. Helicity dependent cross sections,  $\sigma_{v,j,\Omega}(E)$  for (a)  $v=0, j=1$ , (b)  $v=0, j=2$ , (c)  $v=0, j=3$  and (d)  $v=1, j=1$ .

terms in a multipolar expansion of the  $j$  polarization vanish. In Figs. 11 we show the helicity dependent cross section for several initial states of HF. Again there is an important difference between  $v=0$  and 1. While for the ground vibrational state of HF there is an important dependence of the cross section with  $\Omega$ , for  $v=1$  it seems nearly independent.

For  $v=0$ , at low energies nearly all the  $\sigma_{v,j,\Omega}(E)$  show oscillations that are associated with the structure of the transition state, as discussed above. An interesting feature for  $v=0, j=1$  is that the helicity dependent cross section at low energies for  $\Omega=0$  and 1 are in dephase and the average over an isotropic distribution, in Fig. 8, does not show oscillations. At high energies the  $\sigma_{v,j,\Omega=0}(E)$  is much larger than that for  $\Omega=1$ , for  $j=1$ , which suggests that the most favorable initial relative orientation between reactants is approximately collinear. For  $j=2$  and 3 this fact is not so clear, but there is a tendency that the helicity dependent cross section increases with decreasing  $\Omega$ , which suggests that, in general, the reaction efficiency increases when the angular momentum vector  $\mathbf{j}$  is nearly perpendicular to the relative velocity vector between reactants. This implies, again, that the reaction is enhanced when the HF internuclear vector  $\mathbf{r}$  is initially nearly parallel to the velocity between reactants for  $v=0$ .

Recently the stereodynamics of the Li+HF collision has been studied at  $J=0$  (Ref. 65) and it was determined that the reaction occurs preferentially at collinear configuration from the F side of the HF molecule. It should be noted, however,

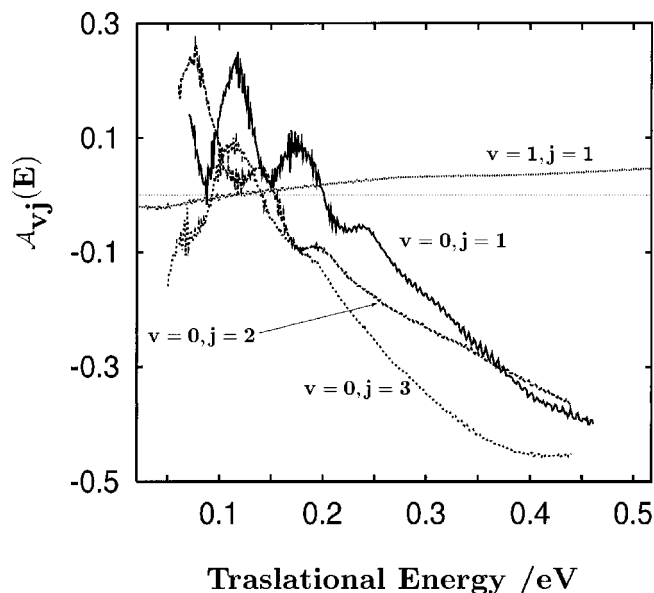


FIG. 12.  $A_{v,j}(E)$ , for several initial states of HF.

that in that treatment,<sup>65</sup> the complete  $S$  matrix, calculated using a different PES,<sup>16</sup> is transformed to the so-called *steredirected* representation, which involves a summation over several initial rotational states of HF. Thus, such a conclusion does not properly correspond to a particular initial  $j$  value of the reactants and the comparison with the results presented in this work (corresponding to a well determined value of  $j$ ) is not clear.

A clearer way to show this fact is provided by the  $A_{v,j}(E)$  parameter defined in Eq. (10), as we show in Fig. 12. All the initial rotational states for  $v=0$  show the same behavior, some oscillations at low energy associated with the structures of the transition state, and at higher energies the  $A_{v,j}(E)$  parameter tends to a value close to  $-0.5$ . Using the semiclassical analog, this value corresponds to an averaged angle between  $\mathbf{j}$  and  $\mathbf{k}$  of approximately  $70^\circ$ .

However, for  $v=1, j=1$ ,  $A_{v,j}(E)$  is close to zero, which indicates that the reaction cross section does not strongly depend on the initial orientation, and at high energies  $\sigma_{v,j,\Omega=1}$  is larger than  $\sigma_{v,j,\Omega=0}$ , i.e., the reaction has a certain preference to occur for  $\mathbf{r}$  perpendicular to the relative velocity. This situation is the opposite to what happens in  $v=0$ , and indicates certain differences in the reaction mechanism between the two vibrational levels. In this regard, there are several experimental studies on the steric effects in the Li+HF( $v=1, j=1$ ) collision<sup>46,30</sup> in which it was determined that the ratio  $\sigma_y^-/\sigma_z^-$  (analog to  $\sigma_{\Omega=1}/\sigma_{\Omega=0}$  in the present treatment) is  $1.8 \pm 0.4$  at a translational energy of 0.42 eV. The calculated ratio in the present case at the same energy is 1.1, lower than the experimental value but it shows the same behavior, i.e., in  $v=1$  the reaction has a certain preference to occur for  $\mathbf{r}$  perpendicular to the relative velocity.

These differences in the stereodynamics of the reaction in  $v=0$  and 1 clarify the reaction dynamics in the following way. The reaction needs some vibrational excitation to take place since the saddle point is located at 1.301 Å while the equilibrium distance for  $v=0$  is approximately 0.921 Å. The

translational energy between reactants is more effectively transferred to the HF vibration when the two reactants collide at near collinear configurations, which explains the higher cross section of low  $\Omega$ . As the initial rotational excitation of HF increases the efficiency of the energy transfer decreases, which explains the rotational disruption observed for  $v=0$ . The situation in  $v=1$  is different because the HF has enough vibrational energy to overpass the barrier. Therefore, the cross section is rather independent of the initial orientation between reactants and only shows a slight preference at angular configurations where the saddle point is more easily achieved, as is the case for collision at angles close to  $\pi/2$ . Since at  $v=1$  the angular cone of acceptance is already quite large, the cross section is rather independent of the rotational excitation, at least for low  $j$ .

#### IV. CONCLUSIONS

In this work we have studied the reactivity on the Li+HF( $v,j$ ) collision, using a PES recently published by us,<sup>19</sup> for different initial rovibrational states of HF and for different orientations of the rotational vector  $\mathbf{j}$  with respect to relative velocity between reactants. Such a study provides a clear and simple picture about the reaction mechanisms, independently of the final state of the products. In a forthcoming work we shall analyze this point.

The reaction requires a certain vibrational excitation of HF to proceed, and the reactive cross sections for  $v=0$  are 10–50 times smaller than those for  $v=1$ . Once this vibrational  $v=1$  excitation is achieved, the cross section is rather independent of the initial rotational state of HF, as well as of the initial orientation of  $j$ . However, the reaction cross section for  $v=1$  shows a monotonous decrease with translational energy typical in exothermic reactions.<sup>63,64</sup>

For HF initially in  $v=0$ , the situation is much more complicated. At low energies the cross section shows some oscillations associated to the structure of the transition state. Such oscillations remain after the average on the rotational state of HF, and its experimental detection would provide direct information of the PES in the region of the saddle point.

The reaction cross section for  $v=0$  shows an important dependence with the initial rotational state of HF and, mainly, a marked tendency to increase for low values of  $\Omega$ , the projection of  $\mathbf{j}$  with respect to the velocity vector. This means that the reaction efficiency tends to increase when the HF internuclear vector,  $\mathbf{r}$ , is parallel to the relative velocity between reactants. At this collinear configuration is where the energy transfer between translational and vibrational motions is more effective, and therefore as soon as the HF is vibrationally excited the reaction takes place. As the initial rotational excitation of HF increases, the reaction is disrupted, at least for the low  $j$  values studied here.

#### ACKNOWLEDGMENTS

This work has been supported by DGICYT (Ministerio de Educación y Ciencia, Spain) under Grant Nos. PB94-0160 and PB95-0071, and by the European TMR network contract

No. ERBFMRX-CT96-0088. We also want to acknowledge DGICYT and CIEMAT for the use of a CRAY-J90.

- <sup>1</sup>T. J. Odiorne, P. R. Brooks, and J. V. V. Kasper, *J. Chem. Phys.* **55**, 1980 (1971).
- <sup>2</sup>J. G. Pruett and R. N. Zare, *J. Chem. Phys.* **64**, 1774 (1976).
- <sup>3</sup>Z. Kamy and R. N. Zare, *J. Chem. Phys.* **68**, 3360 (1978).
- <sup>4</sup>F. E. Bartoszek, B. A. Blackwell, J. C. Polanyi, and J. J. Sloan, *J. Chem. Phys.* **74**, 3400 (1981).
- <sup>5</sup>M. Hoffmeister, R. Schleysing, F. Stienkemeier, and H. J. Loesch, *J. Chem. Phys.* **90**, 3528 (1989).
- <sup>6</sup>B. A. Blackwell, J. C. Polanyi, and J. J. Sloan, *Chem. Phys.* **30**, 299 (1978).
- <sup>7</sup>M. Hoffmeister, L. Potthast, and H. J. Loesch, *Chem. Phys.* **78**, 369 (1983).
- <sup>8</sup>H. H. Dispert, M. W. Geis, and P. R. Brooks, *J. Chem. Phys.* **70**, 5317 (1979).
- <sup>9</sup>C-K. Man and R. C. Estler, *J. Chem. Phys.* **75**, 2779 (1981).
- <sup>10</sup>R. Zhang, D. J. Rakestraw, K. G. McKendrick, and R. N. Zare, *J. Chem. Phys.* **89**, 6283 (1988).
- <sup>11</sup>P. S. Weiss, J. M. Mestdagh, M. H. Covinsky, B. A. Balko, and Y. T. Lee, *Chem. Phys.* **126**, 93 (1988).
- <sup>12</sup>R. Düren, U. Lackschewitz, and S. Milosevic, *Chem. Phys.* **126**, 81 (1988).
- <sup>13</sup>R. Düren, U. Lackschewitz, S. Milosevic, and H. J. Waldapfel, *J. Chem. Soc., Faraday Trans. 2* **85**, 1017 (1989).
- <sup>14</sup>M. Menéndez, M. Garay, E. Verdasco, and A. Gonzalez-Ureña, *J. Chem. Soc., Faraday Trans.* **89**, 1493 (1993).
- <sup>15</sup>M. Baer, I. Last, and H.-J. Loesch, *J. Chem. Phys.* **101**, 9648 (1994).
- <sup>16</sup>G. A. Parker, A. Lagana, S. Crocchianti, and R. T. Pack, *J. Chem. Phys.* **102**, 1238 (1995).
- <sup>17</sup>F. Gögtas, G. G. Balint-Kurti, and A. R. Offer, *J. Chem. Phys.* **104**, 7927 (1996).
- <sup>18</sup>A. Aguado, M. Paniagua, M. Lara, and O. Roncero, *J. Chem. Phys.* **106**, 1013 (1997).
- <sup>19</sup>A. Aguado, M. Paniagua, M. Lara, and O. Roncero, *J. Chem. Phys.* **107**, 10085 (1997).
- <sup>20</sup>R. Gargano, S. Crocchianti, A. Laganá, and G. A. Parker, *J. Chem. Phys.* **108**, 6266 (1998).
- <sup>21</sup>M. Paniagua, J. M. García de la Vega, J. R. Alvarez-Collado, J. C. Sanz, J. M. Alvarino, and A. Laganá, *J. Mol. Struct.* **142**, 525 (1986).
- <sup>22</sup>M. S. Topaler, D. G. Truhlar, X. Y. Chang, P. Piecuch, and J. C. Polanyi, *J. Chem. Phys.* **108**, 5349 (1998).
- <sup>23</sup>J. D. Barnwell, J. G. Loeser, and D. R. Herschbach, *J. Phys. Chem.* **87**, 2781 (1983).
- <sup>24</sup>M. D. Pattengill, R. N. Zare, and R. L. Jaffe, *J. Phys. Chem.* **91**, 5489 (1987).
- <sup>25</sup>M. P. de Miranda and D. C. Clary, *J. Chem. Phys.* **106**, 4509 (1997).
- <sup>26</sup>M. P. de Miranda, D. C. Clary, J. F. Castillo, and D.E. Manolopoulos, *J. Chem. Phys.* **108**, 3142 (1998).
- <sup>27</sup>Z. Kamy, R. C. Estler, and R. N. Zare, *J. Chem. Phys.* **69**, 5199 (1978).
- <sup>28</sup>H. J. Loesch and F. Stienkemeier, *J. Chem. Phys.* **100**, 740 (1994).
- <sup>29</sup>H. J. Loesch and F. Stienkemeier, *J. Chem. Phys.* **100**, 4308 (1994).
- <sup>30</sup>H. J. Loesch, *Annu. Rev. Phys. Chem.* **46**, 555 (1995).
- <sup>31</sup>C. Maltz, N. D. Weinstein, and D. R. Herschbach, *Mol. Phys.* **24**, 133 (1972).
- <sup>32</sup>D. S. Y. Hsu, N. D. Weinstein, and D. R. Herschbach, *Mol. Phys.* **29**, 257 (1975).
- <sup>33</sup>S. K. Shin, Y. Chen, S. Nkolaisen, S. W. Sharpe, R. A. Beaudet, and C. Wittig, *Adv. Photochem.* **16**, 249 (1991).
- <sup>34</sup>B. Soep, C. J. Whitham, A. Keller, and J. P. Visticot, *Faraday Discuss. Chem. Soc.* **91**, 191 (1991).
- <sup>35</sup>B. Soep, S. Abbés, A. Keller, and J. P. Visticot, *J. Chem. Phys.* **96**, 440 (1992).
- <sup>36</sup>A. Keller, R. Lawruszczuk, B. Soep, and J. P. Visticot, *J. Chem. Phys.* **105**, 4556 (1996).
- <sup>37</sup>K. Liu, J. C. Polanyi, and S. Yang, *J. Chem. Phys.* **98**, 5431 (1993).
- <sup>38</sup>J. C. Polanyi and J.-X. Wang, *J. Phys. Chem.* **99**, 13691 (1995).
- <sup>39</sup>X. Y. Chang, R. Ehlich, A. J. Hudson, P. Piecuch, and J. C. Polanyi, *Faraday Discuss.* **108**, 411 (1997).
- <sup>40</sup>R. Lawruszczuk, M. Elhanine, and B. Soep, *J. Chem. Phys.* **108**, 8374 (1998).
- <sup>41</sup>M. Paniagua, A. Aguado, M. Lara, and O. Roncero, *J. Chem. Phys.* **109**, 2971 (1998).

- <sup>42</sup>R. L. Jaffe, M. D. Pattengill, F. G. Mascarello, and R. N. Zare, *J. Chem. Phys.* **86**, 6150 (1987).
- <sup>43</sup>M. M. L. Chen and H. F. Schaefer III, *J. Chem. Phys.* **72**, 4376 (1980).
- <sup>44</sup>A. Aguado, C. Suárez, and M. Paniagua, *Chem. Phys.* **201**, 107 (1995).
- <sup>45</sup>C. H. Becker, P. Casavecchia, P. W. Tiedemann, J. J. Valentini, and Y. T. Lee, *J. Chem. Phys.* **73**, 2833 (1980).
- <sup>46</sup>H. J. Loesch and F. Stienkemeier, *J. Chem. Phys.* **98**, 9570 (1993).
- <sup>47</sup>R. N. Zare, *Angular Momentum* (Wiley, New York, 1988).
- <sup>48</sup>R. T Pack, *J. Chem. Phys.* **60**, 633 (1974).
- <sup>49</sup>P. McGuire and D. J. Kouri, *J. Chem. Phys.* **60**, 2488 (1974).
- <sup>50</sup>Y. Sun, R. C. Mowrey, and D. J. Kouri, *J. Chem. Phys.* **87**, 339 (1987).
- <sup>51</sup>H. Tal-Ezer and R. Kosloff, *J. Chem. Phys.* **81**, 3967 (1984).
- <sup>52</sup>R. Kosloff, *J. Phys. Chem.* **92**, 2087 (1988).
- <sup>53</sup>W. H. Miller, *J. Chem. Phys.* **61**, 1823 (1974).
- <sup>54</sup>D. H. Zhang and J. Z. H. Zhang, *J. Chem. Phys.* **101**, 3671 (1994).
- <sup>55</sup>Y. Sun, R. S. Judson, and D. J. Kouri, *J. Chem. Phys.* **90**, 241 (1989).
- <sup>56</sup>M. Abramowitz and I. A. Segun, *Handbook of Mathematical Functions* (Dover, New York, 1972).
- <sup>57</sup>J. C. Polanyi and W. H. Wong, *J. Chem. Phys.* **51**, 1439 (1969).
- <sup>58</sup>M. H. Mok and J. C. Polanyi, *J. Chem. Phys.* **51**, 1451 (1969).
- <sup>59</sup>M. Brinkhoff, Diplomarbeit, Universität Bielefeld, 1986.
- <sup>60</sup>N. Sathyamurty, *Chem. Rev.* **83**, 601 (1983).
- <sup>61</sup>H. J. Loesch, *Chem. Phys.* **104**, 213 (1986).
- <sup>62</sup>H. R. Mayne and S. K. Minick, *J. Phys. Chem.* **91**, 1400 (1987).
- <sup>63</sup>R. D. Levine and R. B. Bernstein, *J. Chem. Phys.* **56**, 2281 (1972).
- <sup>64</sup>R. D. Levine and R. B. Bernstein, *Molecular Reaction Dynamics and Chemical Reactivity* (Oxford University Press, New York, 1987).
- <sup>65</sup>J. M. Alvaríño, V. Aquilanti, S. Cavalli, S. Crocchianti, A. Laganà, and T. Martínez, *J. Chem. Phys.* **107**, 3339 (1997).